



This is a repository copy of *Investigation of the distribution of localised and extended states in amorphous MoOx*.

White Rose Research Online URL for this paper:

<https://eprints.whiterose.ac.uk/138827/>

Version: Published Version

Article:

Dizayee, W., Ying, M., Griffin, J. et al. (4 more authors) (2018) Investigation of the distribution of localised and extended states in amorphous MoOx. AIP ADVANCES, 8 (5). 055118. ISSN 2158-3226

<https://doi.org/10.1063/1.5027399>

Reuse

This article is distributed under the terms of the Creative Commons Attribution (CC BY) licence. This licence allows you to distribute, remix, tweak, and build upon the work, even commercially, as long as you credit the authors for the original work. More information and the full terms of the licence here:

<https://creativecommons.org/licenses/>

Takedown

If you consider content in White Rose Research Online to be in breach of UK law, please notify us by emailing eprints@whiterose.ac.uk including the URL of the record and the reason for the withdrawal request.



eprints@whiterose.ac.uk
<https://eprints.whiterose.ac.uk/>

Investigation of the distribution of localised and extended states in amorphous MoO_x

Cite as: AIP Advances **8**, 055118 (2018); <https://doi.org/10.1063/1.5027399>

Submitted: 01 March 2018 . Accepted: 07 May 2018 . Published Online: 18 May 2018

Wala Dizayee, Minju Ying, Jonathan Griffin, Mohammed S. Alqahtani, Alastair Buckley, A. Mark Fox , and Gillian A. Gehring 



View Online



Export Citation



CrossMark

ARTICLES YOU MAY BE INTERESTED IN

[Analytical solution and numerical simulation of the liquid nitrogen freezing-temperature field of a single pipe](#)

AIP Advances **8**, 055119 (2018); <https://doi.org/10.1063/1.5030442>

[Thermal stability and Judd-Ofelt analysis of optical properties of Sm³⁺-doped sodium tellurite glasses](#)

AIP Conference Proceedings **1888**, 020032 (2017); <https://doi.org/10.1063/1.5004309>

[Entomocidal activity of microwave energy & some aqueous plant extracts against Tribolium castaneum Herbst & Trogoderma granarium Everts](#)

AIP Conference Proceedings **1888**, 020005 (2017); <https://doi.org/10.1063/1.5004282>

Don't let your writing
keep you from getting
published!

AIP | Author Services

Learn more today!

Investigation of the distribution of localised and extended states in amorphous MoO_x

Wala Dizayee,^{1,2} Minju Ying,^{1,3} Jonathan Griffin,¹ Mohammed S. Alqahtani,^{1,4} Alastair Buckley,¹ A. Mark Fox,¹ and Gillian A. Gehring^{1,a}

¹*Department of Physics and Astronomy, University of Sheffield, Sheffield S3 7RH, United Kingdom*

²*Department of General Science, Salahaddin University, Erbil, Iraq*

³*Key Laboratory of Beam Technology and Material Modification of Ministry of Education, College of Nuclear Science and Technology, Beijing Normal University, Beijing 100875, P.R. China*

⁴*Department of Physics and Astronomy, King Saud University, Riyadh 11451, Saudi Arabia*

(Received 1 March 2018; accepted 7 May 2018; published online 18 May 2018)

Amorphous films of MoO_x have both structural disorder and also chemical disorder for $x < 3$. We have shown that this disorder can introduce localised states in thin films and have shown that the existence of localised states can be deduced from the XPS data that identifies the relevant occupations of different ionisation states of the Mo ions. This effect, which depends on both the oxygen concentration and the method of fabrication, is more important than electron-electron interactions in producing the observed localisation. We have also shown that magneto-optical dichroism is also a powerful technique to determine the energy distribution of localised and delocalised states. © 2018 Author(s). All article content, except where otherwise noted, is licensed under a Creative Commons Attribution (CC BY) license (<http://creativecommons.org/licenses/by/4.0/>). <https://doi.org/10.1063/1.5027399>

I. INTRODUCTION

Transition metal oxides MoO₃, WO₃, V₂O₅ and TiO₂ have become the subject of great interest recently because of their use for charge injection and hole extraction in organic photovoltaic (OPV) and light-emitting diode (OLED) devices. They have a high transparency for visible light, reasonable carrier mobility, deep lying electronic states and high work functions which give them good overlap with occupied levels of the organic molecules.^{1,2} By chemically tuning the work functions to match the energy of the charge transport state, it is possible to minimize losses that can occur at this interface.^{3–5} Amorphous molybdenum oxide MoO_x is one of the most promising metal oxides for these applications and has been used extensively throughout the field both in OLEDs and OPVs.^{3,6–8,10} It has been shown to give injection of holes without a barrier in OLEDs,⁹ and led to OPV devices with 7.9% efficiency.¹¹ MoO_x has also been found to be very suitable for use as a hole injector in inorganic devices.¹²

The increased interest in amorphous MoO_x makes it important to investigate the distribution of the localised and extended states in the vicinity of the Fermi energy, both experimentally and theoretically. This increased interest in the distribution of the energy of the occupied and empty levels of MoO_x has led us to study these states in more detail using a theoretical analysis of the distribution of the molybdenum oxidation states and also magnetic circular dichroism MCD, which is very sensitive to the existence of localised states, to complement the existing surface science literature.

Bulk MoO₃ is a semiconductor with a band gap of 3eV.⁴ It contains Mo⁶⁺ which has an empty d shell. The valance and conduction bands are predominantly composed of oxygen p states and Mo d states respectively.¹³ The density functional theory gives a good description of the bulk material

^aCorresponding author. Gillian A. Gehring g.gehring@sheffield.ac.uk

however correlation effects which are treated by adding a Hubbard U are necessary in order to get a good understanding of the localised surface states.¹⁵ The other bulk oxide, MoO_2 , is a metal that crystalizes in a monoclinic structure with four MoO_2 formula units per unit cell. The band structure calculations show that there are two low lying orbitals in the conduction band that correspond to the Goodenough t_{11} bands of the d -orbitals.¹⁴ The Fermi level lies in the band of d states corresponding to an average occupation of two d electrons per molybdenum giving an average configuration of d^2 for the Mo^{4+} ions.¹³

In amorphous films of MoO_x where $x < 3$ there are three energies that determine the ratios of the occupancies of the different ionisation states of the Mo ions. These are the interionic transfer between Mo ions that gives rise to the d electron band width W – this would give rise to extended states. There are two effects that tend to give deviations from simple band theory and in some cases localise the electrons: one is the spread of local energies, Δ , that occur due to the structural disorder and the lack of oxygen stoichiometry in the amorphous film and the other is the repulsion between electrons at the same Mo ion, the Hubbard U .^{16,17} If the structural disorder is important the Mo ions in particularly favourable or unfavourable positions will have unusually low or high oxidation as the electrons will cluster on the most favourable sites; whereas the electron–electron repulsion will favour the configurations with low site occupancy.

In this work we bring together x-ray photo-electron spectroscopy, XPS, and magnetic circular dichroism, MCD, measurements with a first principles statistical treatment of the occupancy of Mo atomic energy levels in order to elucidate the nature of the electronic structure of differently fabricated MoO_x films.¹⁸ We find remarkable agreement with a model based on non-interacting band electrons, valid for extended states, for certain films but large disagreements for others, indicating that substantial numbers of localised states exist in some films. In the latter case, a small polaron method becomes appropriate for an understanding of the transport and the optical properties.¹⁹ Support for this comes from optical absorption and magnetic circular dichroism measurements which is crucial for determining if the electrons at the Fermi level are in localised states.

The fabrication of our samples and the experimental techniques for measuring the distribution of the ionisation states of the Mo ions and MCD are described in section II and in section III we describe our understanding of the electronic states of MoO_3 , MoO_2 and amorphous MoO_x . These can be understood in terms of band theory for the stoichiometric compounds and for amorphous MoO_x in terms of a disordered dominated regime in which a small polaron description is more appropriate.¹² We discuss the possible types of density of states that would be expected for a film with a mixture of occupied localised and extended states and relate this to the observed optical properties in section IV. We find that the optical loss was dominated by the scattering but that the MCD allowed us to determine whether a film had localised or extended states at the Fermi level. The conclusions are given in Section V.

II. EXPERIMENTAL METHODS

A. Deposition of amorphous molybdenum oxide films

The MoO_x films studied here were deposited via reactive magnetron sputtering from a molybdenum metal target using a blend of argon (99.998%) and oxygen (99.9995%) on either sapphire (for MCD experiments) or Si $\langle 100 \rangle$ (for XPS measurements) substrates. Prior to film deposition substrates were cleaned in an ultrasonic bath with hot de-ionized water followed by isopropanol and then UV/ozone treatment to remove organic residue. For most XPS measurements film thickness was 15 nm to mirror thicknesses used as electrode layers in solar cells. For MCD larger signals are needed and film thickness of $\sim 50\text{nm}$ were used. The argon:oxygen (Ar/O) ratios are given in Table I. An overall deposition pressure of 5×10^{-2} mbar was maintained and the power coupled into the plasma was kept at a constant value of 200 W.

B. Measurement of the oxidation states of Mo

The state of ionisation of the Mo ions in the films was deduced from the measured XPS from the 3d levels. It is known from other work on epitaxial thin films that amorphous MoO_x will contain

TABLE I. The comparison of the occupations of the different oxidation states of the Mo ions in MoO_x determined by XPS and deduced from band theory for bands *s* bands. Data for films that fit the statistical theory within 5% are shaded green, those with moderate deviation were shaded pink and those with very large deviations are shaded orange.

Film	Method. Thickness. Growth conditions. Number of bands in model, <i>s</i> . [Source].	<i>x</i>	<i>n</i>	% of each Mo ion from:	<i>P</i> ₀	<i>P</i> ₁	<i>P</i> ₂	<i>P</i> ₃	<i>P</i> ₄	<i>P</i> ₅	<i>P</i> ₆
					Mo ⁶⁺	Mo ⁵⁺	Mo ⁴⁺	Mo ³⁺	Mo ²⁺	Mo ⁺	Mo
1	Sputtering. 15 nm. Ar: O ₂ ratio = 80:20 <i>s</i> = 2 [Griffin ²³]	2.87	0.26	Expt	74	25	1	0	0	0	0
				Band	75	23	2	-	-	-	-
2	Sputtering. 15 nm. Ar: O ₂ ratio = 85:15. <i>S</i> = 4. [Griffin ²³]	2.41	1.2	Expt	26	40	25	10	0	0	0
				Theory	25	41	26	7	1	-	-
3	Deposited on V <i>s</i> = 2. [Greiner ⁴]	2.25	1.5	Expt	7	36	57	0	0	0	0
				Theory	6	36	56	-	-	-	-
4	Sputtering. 15 nm. Ar: O ₂ ratio = 85:15 <i>s</i> = 2 [Griffin ²³]	2.35	1.3	Expt	20	48	15	17	0	0	0
				Theory	21	40	29	9	1	-	-
5	Evaporation. <i>s</i> = 2. [Vasilopoulou ²⁴]	2.7	0.7	Expt	50	30	20	0	0	0	0
				Theory	42	46	12	-	-	-	-
6	Sputtering. 15 nm. Ar:O ₂ ratio = 90:10 <i>s</i> = 4. [Griffin ²³]	2.21	1.58	Expt	26	15	35	24	0	0	0
				Theory	13	35	34	15	2	-	-
7	Sputtering. 50 nm. Ar:O ₂ ratio = 87:13. <i>s</i> = 2. [This work]	2.7	0.7	Expt	56	20	24	0	0	0	0
				Theory	42	46	12	-	-	-	-
8	Sputtering. 50 nm. Ar:O ₂ ratio = 17:3. <i>s</i> = 4. [This work]	1.6	2.8	Expt	14	9	8	16	53	0	0
				Theory	1	8	26	41	24	-	-

a mixture of ionisation states with known doublet peak locations.^{13,20–24} However this procedure of determining the state of ionisation from the XPS spectrum is controversial because if there is substantial occupancy of free electron states then a doublet is seen due to there being both a screened and an unscreened peak for a single value of the ionisation of the Mo ion.¹³ We believe that for values of *x* in the range $2.3 < x < 3$ the number of carriers is sufficiently small so that screening is ineffective and for smaller values of *x* the substantial spatial disorder has rendered the screening from the Mo 4*d* electrons ineffective. Hence we are justified in assuming that each peak in the XPS spectrum corresponds to a different ionisation state of the Mo ions.

Following deposition, samples were briefly (5 minutes) exposed to air while being transferred to a Kratos ultra AXIS photoelectron spectrometer and XPS measurements were taken of the Mo3*d* and C1*s* peaks using the Al *k*- α emission line at 1486.6 eV. The Mo 3*d* peak was fitted with doublet peaks with a fixed spacing of 3.15 eV. Following Shirley background correction the intensities of the doublets were fitted to the different oxidation states of Molybdenum, the first peak for the Mo⁶⁺, Mo⁵⁺, Mo⁴⁺, Mo³⁺, Mo²⁺ and Mo¹⁺ are at 235.9 eV, 234.7 eV, 233.5 eV, 232.8 eV, 231.6 eV and 230.9 eV respectively. The results of the fitting of are given in Table I and example XPS fits for samples are given in figure 1. We note that there is an error of ~5% in the estimation of the concentrations of the ionisation states of the Mo ions.

C. Optical techniques

The absorption spectra of the films between 1.7 and 4.5 eV were taken by measuring the transmission using chopped light from a xenon lamp and a monochromator with a photo-multiplier tube detector. This was analysed in terms of the intensity lost in the film to give a loss coefficient, α ; this incorporates real absorption, scattering from the front and back surfaces and also from grain

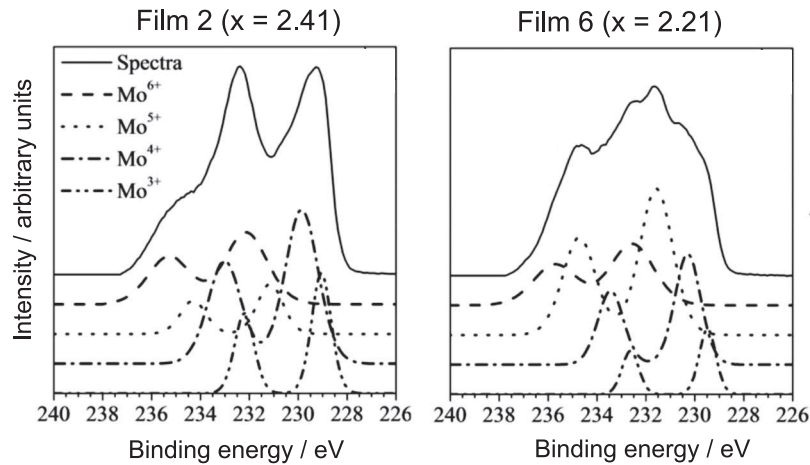


FIG. 1. Examples of fitted XPS spectra for thin films of MoO_x where $x = 2.41$ (left plot) and $x = 2.21$ (right plot). The data is a re-analysis of samples described in reference 23. The contributions to the overall spectra from Mo ions of different oxidation state are shown offset below the measured spectra.

boundaries in the film. MCD spectra were taken in the same energy range using a photoelastic modulator.^{25,26} The measurements were taken at room temperature in an applied magnetic field of 1.8 T and we detect a signal from the occupied states that are spin polarised by this applied magnetic field.²⁷ The upper limit of the energy on our MCD plots was determined by the point where the films begin to absorb strongly; at this point the total transmitted intensity is too low, and we cannot record the MCD accurately. The data from the sapphire substrates was also recorded. Sapphire is transparent and therefore has a very low MCD when measured in degrees/cm. However, as it is so much thicker than the film, its contribution is very important and it is subtracted from all our measurements.^{27,28}

III. STATISTICAL MODEL AND COMPARISON WITH XPS DATA

As oxygen is removed from MoO₃ a defect band is formed below the conduction band.⁴ This is made up predominantly of the two t_{11} Goodenough bands that are seen in the band structure of the ordered compounds, MoO₃ and MoO₂.^{13,14} These bands are formed from localised Mo-O bonds so have a small dispersion over most of the Brillouin zone. Localisation occurs when the fluctuations in the local potential become comparable with the band width¹⁶ and so amorphous films of MoO_x are particularly prone to having a localisation transition.²³

If the electrons are in band states then the occupation of the states is given by a statistical model.¹⁸ This model assumes that electrons move independently in extended states that are occupied up to the Fermi level. The model is valid if the band width is large compared with the variation in the local potentials and the one-site electronic repulsion. In the statistical model the probability of local occupancy of r non-interacting electrons on a given site, P_r^{band} , is given by the binomial formula in terms of the average occupancy, n , and the total number of available atomic states, s .

$$P_r^{band} = \frac{s!}{r!(s-r)!} \left(\frac{n}{s}\right)^r \left(1 - \frac{n}{s}\right)^{s-r}. \quad (1)$$

In this work we investigate the validity of this model when electrons are in extended states in amorphous MoO_x. The local occupations of the Mo ions, P_r^{exp} , are measured using XPS where measurements indicating Mo⁶⁺ correspond to $r = 0$, Mo⁵⁺ correspond to $r = 1$, etc. so that the state with r electrons is characterised by Mo^{6-r}. We consider the whether the observed distribution of the occupation numbers of Mo ionic states correspond to those expected for a band containing s delocalised electrons. The total number of occupied states, n , is given below;

$$n = \sum_{r=1}^s r P_r^{\text{exp}}. \quad (2)$$

The value of n depends on the method of fabrication, the thickness of the films as well as the amount of oxygen used in the deposition as is clear from the results from the literature and the current study shown in Table I. The oxygen content in MoO_x , given by x , is related to the total number of electrons in the Mo d states, n , by $x = \frac{1}{2}(6 - n)$.

The values of P_r^{band} is calculated using the experimentally determined value of n , obtained using equation (2) and the experimental values P_r^{exp} and the smallest value of s consistent with the observed occupations obtained by XPS. (Actually the values of P_r^{band} are actually rather insensitive to the value of s that was used as a larger value of s gives a very similar fit.)

In Table I data from our samples are compared with data from other films taken from the literature. For each film we give the experimentally measured values of P_r^{exp} and the values of n and x deduced using equation (2).

We did not include data for films with low occupation $n < 0.2$ because they only have a very small probability of occupation of Mo^{4+} and if there is only occupation of two states, Mo^{5+} and would Mo^{4+} the results would be fitted by any theory. The agreement for the films **1-3** with the model including bands with four or two fold degeneracy are really surprisingly good, bearing in mind that the expected accuracy of the occupations found from XPS data is $\pm 5\%$. We can conclude that the films of MoO_x **1,2,3** have substantially *all* the electrons in extended states.

By contrast if there are strong local attractive potentials at some Mo sites these can have a large number of bound states so the values of occupation, P_r^{exp} , will not be given by equation (1) but will be substantially larger. Substantial deviations between the experimentally observed occupation numbers and those predicted by band theory are seen for films 4-8, those with deviations between 6% and 19% are shaded pink and those with deviations greater than 19% are orange. We see that the experimentally observed occupation of ions in the states with the highest number of d electrons are larger than predicted by the statistical theory. Our observations also exclude the possibility that the localisation is due to electron-electron repulsion because this interaction would tend to inhibit the states with higher electron occupation which is the reverse of what is observed here. We conclude that the occurrence of localised states are due to the random potentials. This is not surprising in view of the fact that these films were both amorphous and non-stoichiometric.

Since deviations from the band model are caused by the random nature of the films, it is not surprising that it depends on the non-stoichiometry but also the method of deposition. Films **5** and **7** have a small carrier density but appear to have some localised states. It is significant that film **5** was grown by a different technique and that film **7** was very much thicker than films **1-6**. The fact that the film quality depends on thickness was seen for films on MoO_x where $x \sim 2.9$.²⁹

Note that while films **2** and **4** appear to have been deposited under the same conditions the films have slightly different values of x and values of P_r^{exp} particularly for $r=2$ and 3. In the regimes using 15 – 20% partial pressure of oxygen in the sputtering the history of the target is critical in determining the properties of the film.²³

IV. USING OPTICAL PROPERTIES TO INVESTIGATE THE ELECTRONIC STATES OF MoO_x

A. Absorption: Theoretical considerations

We first consider the nature of the states in films with a substantial number of localised states in the low energy portion of the band. There will be a definite energy separating the localised states, ε_L , occurring in a low energy tail of the density of states and extended states that occur at higher energies. The occupied states lie below the Fermi energy, ε_F , so there are two possible scenarios corresponding to situations where there are extended states at the Fermi level for which $\varepsilon_L < \varepsilon_F$, and where $\varepsilon_L > \varepsilon_F$ so that the states at the Fermi level are localised. These are shown schematically in Fig. 2.

The different optical transitions in which an electron is transferred from below to above the Fermi level for the densities of states shown in figure 2 are: (i) from one localised state to another localised

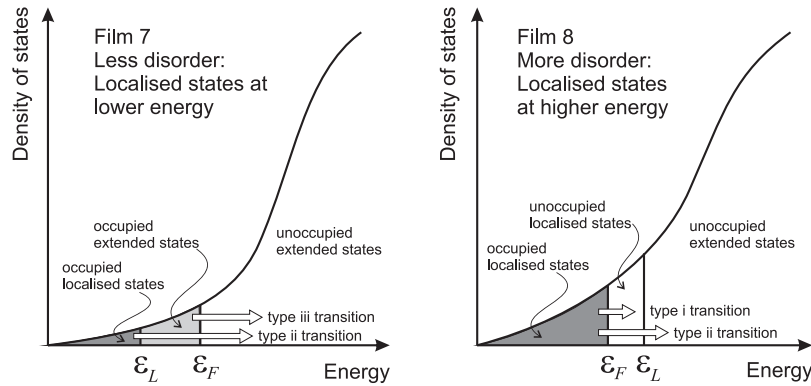


FIG. 2. Schematic density of states for the defect states showing the position of the Fermi level relative to the localisation edge for film **7** where there is less disorder and the Fermi level lies above the localisation edge and film **8** where there is a large amount of disorder and the Fermi level lies below the localisation edge.

state – this can only occur for films of the type of film **8** shown above; (ii) from a localised state to an extended state and (iii) from one extended state to another extended state– this can only occur for films of the type of film **7** shown above.

Transitions of type (i) require the proximity of two ions with localised states with one below and one above the Fermi level so that polaron transitions of the type $d^1 d^2 \rightarrow d^2 d^1$, an electron is exchanged between two localised states, or $d^2 d^3 \rightarrow d^1 d^4$, where the final state contains differently charged ions. These are all polaron transitions¹⁹ because the radius of a Mo ion depends on its charge so the lattice is involved in the transition.

Transitions of type (ii) between a localised state at low energy to a higher energy extended state can occur readily, these correspond to the ionisation of a localised defect and these intensities will be strong because the localised states will have extended states, at a higher energy, in their locality.

Transitions of type (iii) are between two extended states; this would be between two different bands and conserve wavenumber with in a uniform system but here the condition on the wave number is relaxed because of the disorder.

If the Fermi level occurs within the localised states then transitions are of type (i) for energies E satisfying $0 < E < \epsilon_L - \epsilon_F$ and of both type (i) and type (ii) for $E > \epsilon_L - \epsilon_F$. A different scheme occurs if the Fermi level lies above the localised states in the region of extended states; for low energies all the transitions are of type (iii) for $0 < E < \epsilon_F - \epsilon_L$ and of both type (ii) and (iii) for $E > \epsilon_F - \epsilon_L$.

We have made optical measurements on the two films with thicknesses $\sim 50\text{nm}$; films **7** and **8**. Both of these film may be identified as having some localised states because the occupation numbers show significant deviations from those predictions by band theory as shown in Table I. The deviations for film **8** are considerably larger than for films **7** and involve a higher number of electrons.

If the Fermi level occurs within the localised states then transitions are of type (i) for energies E satisfying $0 < E < \epsilon_L - \epsilon_F$ and of both type (i) and type (ii) for $E > \epsilon_L - \epsilon_F$. A different scheme occurs if the Fermi level lies above the localised states in the region of extended states; for low energies all the transitions are of type (iii) for $0 < E < \epsilon_F - \epsilon_L$ and of both type (ii) and (iii) for $E > \epsilon_F - \epsilon_L$.

The loss coefficient, α , is shown in Figure 3(a): this includes both absorption and scattering. We see that the value of α is small and almost independent of temperature for film **7** and but considerably larger for film **8** where there is a much larger number of carriers 2.8 compared with 0.7 for film **7**. The absorption gets very strong above $E=3.7\text{eV}$ and 3.9eV for films **8** and **7** respectively – this corresponds to the region where the optical conductivity rises sharply in MoO_2 .^{30,31} Both the absorption and the scattering are larger for the film **8** because it has a higher density of oxygen defects and a larger number of carriers in gap states. From this data it is not possible to separate the effects of absorption from scattering however this is done when we consider the MCD where scattering does not contribute to the result.

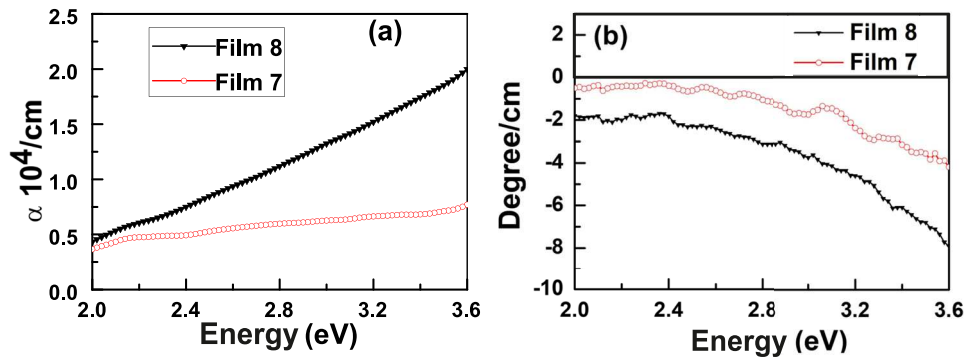


FIG. 3. (a) The loss coefficient, α , of films 7 and 8 (b) the MCD of the films as corrected for contributions from the substrate and from the polar Kerr effects as explained in Ref. 28.

B. Magnetic circular dichroism (MCD) spectra

An applied magnetic field will split of all the electronic states in the material by energies of the order of $\mu_B|B|$. This results in an induced magnetisation due to the unequal populations of the spin and orbital states in the partially occupied levels. The spin orbit coupling produces unequal orbital polarisations as a result of this spin polarisation. The intensities of the absorption observed along a direction parallel to the direction of the field will be polarised σ_+ or σ_- due to this unequal orbital population which affects the oscillator strength for $\Delta m = \pm 1$ in electric dipole transitions.³² Historically this type of MCD spectrum is known as ‘paramagnetic’ and the MCD spectrum follows that of the absorption spectrum modulated by the strength of the Zeeman splittings and the spin orbit interaction in the electronic states that are involved in the transition. In a nonmagnetic material in an induction of 1.8 T, as used in our experiments, at room temperature the population imbalances are small, of the order of 10^{-3} , so this MCD signal is weak but observable. Observation of a ‘paramagnetic’ MCD signal does not imply that a measurement of the bulk magnetisation would yield a paramagnetic response because the small paramagnetism from the gap states might be overwhelmed by the diamagnetic response of the rest of the sample.

There is another type of MCD signal known as a ‘diamagnetic’ signal which can occur in materials with and without partially filled shells. This signal results from the differences in energies of the σ_+ and σ_- transitions because of the Zeeman effect.³² A diamagnetic MCD signal is dispersive over an energy range of $\mu_B|B|$; for the maximum induction used in these experiments, 1.8T, this corresponds to an energy of the order of 10^{-5} eV. This energy is much smaller than the resolution of our apparatus which is about 10^{-2} eV and hence it is not observed in our measurements. This type of spectrum may be observed using a large value of $|B|$.

Hence we are concerned with the polarisability of the occupied states. The susceptibilities of unpaired electrons in localised states will follow a Curie law; whereas the susceptibility of the extended states will be due to Pauli paramagnetism which is proportional to the density of states at the Fermi level. This means that the MCD due to transitions from localised states will be larger than that due to transitions from the extended states. Hence it is important to consider which of the localised states will have an uncompensated spin.

Obviously any localised state on a Mo^{5+} will be magnetic with spin 1/2. If the Mo ions were in perfect octahedra then the lowest state is an orbital triplet, t_{2g} . This means it would be in a state $S = 1$ for Mo^{4+} and $S = 3/2$ for Mo^{3+} . If the crystal field energies due to the distortion of the octahedron are large compared with the atomic exchange then the spins will become $S = 0$ for Mo^{4+} and $S = 1/2$ for Mo^{3+} . The size of the octahedral crystal field determines if the spin state of the Mo^{2+} ion is high, 2, intermediate, 1, or low, 0. Thus all the Mo^{5+} and Mo^{3+} ions will have magnetic localised states and it is likely that most of the Mo^{4+} and some of the Mo^{2+} will be magnetic too.

We consider first the relation between the loss coefficient and the MCD for film 7 ($2.2 < x < 2.4$) as shown in Figs. 2(a) and (b). The loss coefficient, α , includes the scattering from the back and front surfaces of the film and from inhomogeneities in the film as well as the real absorption of the film.

There is a small rise in α between 2eV and 3.6eV, while the MCD is close to zero for $2.0 < E \leq 2.5$ eV and then drops to a value of ~ -4 deg/cm at an energy of 3.6eV. Thus it appears that the transitions are of type (iii) for $E < 2.5$ eV and type (ii) for $E > 2.5$ eV which implies that the Fermi level lies in a region of extended states in film **7** as shown in Fig. 1(b). The strong MCD in the range $E > 2.5$ eV in spite of the rather weak absorption is an indication of the strongly magnetic localised states implying that the Mo^{4+} ions are in $S=1$ states rather than $S=0$.

We now consider the absorption and MCD for film **8**. The absorption is considerably larger than for film **7** as expected because of the much larger number of the occupied states in the gap. The MCD is finite but approximately independent of energy for $E < 2.3$ eV and then falls rapidly to -8 degrees/cm for $E > 2.3$ eV. The region for $E < 2.3$ eV will be type (i) showing that the density of states is approximately independent of energy as occurs in other disordered systems^{33,34} and the weaker effect when transitions are of the polaron type. In the higher energy region, $E > 2.3$ eV the strong MCD with a similar energy dependence indicates that this is a type (ii) transition. This indicates that film **A** has localised states at the Fermi level.

V. CONCLUSIONS

Through careful analysis of XPS data from existing studies and from samples prepared for this study we have shown that MoO_x can be prepared with either localised or extended electronic states. We base our conclusion on the exceptional precision with which the statistical model fits for a subset of samples. We found that for x between 2 and 2.8 the level of oxidation did not solely determine the electronic regime with films of both types being found. Our findings open the door for more detailed understanding of the electronic structure and functions of amorphous MoO_x .

In this study we have compared two films of MoO_x made via reactive magnetron sputtering. The two films had different oxygen content both less than 3 with occupations of the Mo d states of 0.6 and 2.8.

The technique of MCD enabled us to distinguish between a loss of transmission due to scattering and one due to real absorption in these samples where the photoluminescence signal is quenched due to disorder.

We used the different occupations of the ionisation states to show that both films had some occupancy of localised states – although this was much larger for the film with d occupancy of 2.8. The MCD measurements were used to show that in the case of the film with d occupancy of 0.6 the localised states were in the band tail well below the Fermi energy. However in the film with d occupancy of 2.8 the localised states persisted above the Fermi energy.

ACKNOWLEDGMENTS

M. Y. thanks the Fundamental Research Funds for the Central Universities and the National Natural Science Foundation of China under Grant no. 11675280. The measurements of optical absorption and MCD were taken on apparatus initially funded by the UK Engineering and Physical Sciences Research EP/D070406/1. Sample preparation was funded by UK Engineering and Physical Sciences Research under research grant EP/H049452/1.

- ¹ S. Tokito, K. Noda, and Y. Taga, "Metal oxides as a hole-injecting layer for an organic electroluminescent device," *J. Phys. D* **29**, 2750 (1996).
- ² V. Shrotriya, G. Li, Y. Yao, C.-W. Chu, and Y. Yang, *Appl. Phys. Lett.* **88**, 073508 (2006).
- ³ S. Braun, W. R. Salaneck, and M. Fahlman, *Advanced Materials* **21**, 1450 (2009).
- ⁴ M. T. Grenier, M. G. Helander, W. M. Tang, Z. B. Wang, J. Qiu, and Z. H. Lu, *Nature Mat.* **11**, 76 (2012).
- ⁵ J. Meyer, S. Hamwi, M. Kröger, W. Kowalsky, T. Riedl, and A. Kahn, *Adv. Mater.* **24**, 5408 (2012).
- ⁶ M. Vasilopoulou, L. C. Palilis, D. G. Georgiadou, A. M. Douvas, P. Argitis, S. Kennou, L. Sygellou, G. Papadimitropoulos, I. Kostis, N. A. Stergiopoulos, and D. Davazoglou, *Adv. Funct. Mater.* **21**, 1489 (2011).
- ⁷ M. Vasilopoulou, A. Soultati, D. G. Georgiadou, T. Stergiopoulos, L. C. Palilis, S. Kennou, N. A. Stathopoulos, D. Davazoglou, and P. Argitis, *J. Mater. Chem. A* **2**, 1738 (2014).
- ⁸ Y. Sun, C. J. Takacs, S. R. Cowan, J. H. Seo, X. Gong, A. Roy, and A. J. Heeger, *Adv. Mater.* **23**, 2226 (2011).
- ⁹ M. Vasilopoulou, L. C. Palilis, D. G. Georgiadou, S. Kennou, I. Kostis, D. Davazoglou, and P. Argitis, *Appl. Phys. Lett.* **100**, 013313 (2012).
- ¹⁰ J. Griffin, D. C. Watters, H. Yi, A. Iraqi, D. G. Lidzey, and A. R. Buckley, *Adv. Energy Mat.* **3**, 903 (2013).
- ¹¹ Y. Zou, J. Holst, Y. Zhang, and R. J. Holmes, *J. Mater. Chem. A* **2**, 12397 (2014).

- ¹² C. Battaglia, X. Yin, M. Zheng, I. D. Sharp, T. Chen, S. McDonnell, A. Azcatl, C. Carraro, B. Ma, R. Maboudian, R. M. Wallace, and A. Javey, *Nano Lett.* **14**, 967 (2014).
- ¹³ D. O. Scanlon, G. W. Watson, D. J. Payne, G. R. Atkinson, R. G. Egdell, and D. S. L. Law, *J. Phys. Chem. C* **114**, 4636 (2010).
- ¹⁴ J. B. Goodenough, *Czech. J. Phys.* **17**, 304 (1967).
- ¹⁵ R. Coquet and D. J. Willock, *Phys. Chem. Chem. Phys.* **7**, 3819 (2005).
- ¹⁶ P. W. Anderson, *Phys. Rev.* **109**, 1492 (1958).
- ¹⁷ J. Hubbard, *Proc. Roy. Soc. Ser. A* **276**, 238 (1963); **277**, 237 (1964).
- ¹⁸ G. van de Laan and M. Taguchi, *Phys. Rev. B* **82**, 045114 (2010).
- ¹⁹ A. Siokou, G. Leftheriotis, S. Papaefthimiou, and P. Yianoulis, *Surface Science* **482-485**, 2994 (2001).
- ²⁰ M. Yamada, J. Yasumaru, M. Houalla, and D. M. Hercules, *J. Phys. Chem.* **95**, 7037 (1991).
- ²¹ V. Bhosle, A. Tiwari, and J. Narayan, *J. Appl. Phys.* **97**, 083539 (2005).
- ²² Z. Zhang, Y. Xiao, H. X. Wei, G. F. Ma, S. Duhm, Y. Q. Li, and J. X. Tang, *Appl. Phys. Express* **6**, 095701 (2013).
- ²³ J. Griffin, "Transition metal oxides and their use as hole extraction materials in organic photovoltaic devices," PhD thesis. University of Sheffield (2014).
- ²⁴ M. Vasilopoulou, A. M. Douvas, D. G. Georgiadou, L. C. Palilis, S. Kennou, L. Sygellou, A. Soultati, I. Kostis, G. Papadimitropoulos, D. Davazoglou, and P. Argitis, *J. Am. Chem. Soc.* **134**, 16178 (2012).
- ²⁵ K. Sato, *Jap. J. of Appl. Phys.* **20**, 2403 (1981).
- ²⁶ W. P. van Drent and T. Suzuki, *J. Mag. Magn. Mater.* **175**, 53 (1997).
- ²⁷ M. Ying, W. Dizayee, Z. X. Mei, X. L. Du, A. M. Fox, and G. A. Gehring, *J. Phys. D: Appl. Phys.* **48**, 255502 (2015).
- ²⁸ W. Dizayee, M. Ying, A. Mark Fox, and G. A. Gehring, *arXiv: 1505.03458* (2015).
- ²⁹ P. A. Spevack and N. S. McIntyre, *J. Phys. Chem.* **97**, 11020 (1993).
- ³⁰ L. L. Chase, *Phys. Rev. B* **10**, 2226 (1974).
- ³¹ M. A. K. L. Dissanayake and L. L. Chase, *Phys. Rev. B* **18**, 6872 (1978).
- ³² G. B. Scott, D. E. Lacklison, H. I. Ralph, and J. L. Page, *Phys. Rev. B* **12**, 2562 (1975).
- ³³ K. J. Saji and M. K. Jararaj, *Phys. Stat. Sol. (A)* **205**, 1625 (2008).
- ³⁴ I. Sakata and M. Yamanaka, *J. Appl. Phys.* **97**, 103707 (2005).